Coordination Chemistry Reviews 255 (2011) 2882–2891

Contents lists available at ScienceDirect

Coordination Chemistry Reviews

journal homepage: www.elsevier.com/locate/ccr

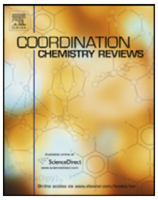

Review

Redox chemistry of aquatitanium(II), $Ti^{2+}(aq)$☆

Edwin S. Gould*

Department of Chemistry and Biochemistry, Kent State University, P.O. Box 5190, Kent, OH 44242, USA

Contents

ARTICLE INFO

Article history:
Received 7 February 2011
Accepted 13 June 2011
Available online 22 July 2011

Keywords:
Aquatitanium(II)
Oxidation
Reduction

ABSTRACT

The growth of industrial interest, since 1960, in organic derivatives of titanium(II) (such as alkoxides and cyclopentadienyls) stands in contrast to the elusive nature of this state as its salts in polar media. The preparation, in 2003, of triflates of this ion in $HF–CF_3SO_3H$ made solutions of this cation conveniently available, although such preparations contained Ti(IV) as well. The standard potential for the Ti(II,III) couple remains in doubt. Rates of reduction, using Ti(II), of quinones and complexes of Co(III), Ru(III) and Fe(III) are often very similar to rates for reductions by Ti(III). A number of Ti(II) reductions are catalyzed by Ti(IV). Depending on the oxidant and the medium, such catalysis may involve: (a) the rapid formation of a 1:1 Ti(II)–Ti(IV) complex ($K_f = 400\,M^{-1}$ at 22 °C); (b) slow comproportionation, yielding Ti(II) (Ti(II) + Ti(IV) → 2Ti(III)); or (c) slow conversion of Ti(II)(aq) to a more reactive coordinatively unsaturated transient. Trapping experiments with $[Co(NH_3)_5Br]^{2+}$ demonstrate that the oxidations of Ti(II) using Cr(VI) or Cr(IV) proceed via $1e^-$ transactions.

1. Introduction

For more than 160 years after the discovery of titanium in 1791, the chemistry of this element was concerned mainly with the metal itself and its 3+ and 4+ states. The report, in 1955, of titanium-based Ziegler catalysts for the polymerization of alkenes [1] triggered a remarkable growth of low-valent titanium chemistry, and an impressive array of organotitanium compounds has been described during the intervening half-century [2], many of these derived from the dipositive state. In addition, titanium(II)-cyclopentadienyls and alkoxides have exhibited versatility in organic conversions [3].

Nevertheless, relatively little attention has been devoted to the "parent" Ti(II) entity, the aquatitanium(II) cation, $Ti^{2+}(aq)$. Reports by Forbes and Hall [4a] and Olver and Ross [4b] indicated that this cation readily reduces aqueous solutions to H_2 at low pH, thus complicating conventional methods of handling. Among the 3d-block dipositive cations, Ti(II) is undoubtedly the most elusive.

However, facile preparations of green solutions of this state in HF–triflic acid mixtures were described in 2003 by Kolle and Kolle [5], and Yang has noted that 0.1 M Ti(II) solutions so generated survive for 12 h at room temperature under argon [6].

Titanium(II) solutions prepared in this manner contain equivalent concentrations of Ti(IV) and a HF/Ti(II) ratio approximately 6:1. Although such preparations are strongly acidic, Ti(IV) is present mainly as $[TiF_6]^{2-}$. In analogy with other (smaller) 3d dipositive cations [7] conversion of Ti(II) to a fluoro complex in these solutions is expected to be slight. Visible spectra recorded by Yang [6] feature $\varepsilon_{660}^{max} = 3.5$ and $\varepsilon_{430}^{max} = 6.0 M^{-1} cm^{-1}$, in contrast to lower values (0.5 and $0.8\,M^{-1}\,cm^{-1}$) documented by the Kolles [5].

☆ All potentials in this review are listed in reference to the standard NHE electrode.

* Tel.: +1 330 672 2267.
E-mail address: amcphers@kent.edu

0010-8545/$ – see front matter © 2011 Elsevier B.V. All rights reserved.
doi:10.1016/j.ccr.2011.06.006

Table 1
Rate laws and kinetic parameters for oxidations of $Ti^{2+}(aq)$.[a]

Ox	Rate law	Parameters
$[CoA_5F]^{2+}$[b]	$k\,[CoA_5F]\,[Ti^{II}]$	$k = 7.8 \times 10^2\ M^{-1}\,s^{-1}$
$[CoA_5Cl]^{2+}$	$k\,[CoA_5Cl][Ti^{II}]$	$k = 0.26\ M^{-1}\,s^{-1}$
$[CoA_5(H_2O)]^{3+}$	$k\,[CoA_5Aq][Ti^{II}]/[H^+]$	$k = 3.2 \times 10^{-2}\ s^{-1}$
$[Co(C_2O_4)_3]^{3-}$	$k\,[CoOx_3][Ti^{II}]$	$k = 62\ M^{-1}\,s^{-1}$
$[NDS^\bullet]^{2-}$[c]	$k\,[NDS^\bullet][Ti^{II}]$	$k = 5.3 \times 10^3\ M^{-1}\,s^{-1}$
I_3^-	$\frac{I^-[Ti^{II}](k_0+k'K[I^-])}{(1+K[I^-][H^+])}$	$k_o = 3.1\ s^{-1}$; $k' = 0.052\ s^{-1}$; $K = 7 \times 10^2\ M^{-1}$

[a] Reactions at 22 °C, $\mu = 0.5$ M; $[H^+] = 0.1–0.5$ M.
[b] $CoA_5 = (NH_3)Co(III)$.
[c] Nitrosodisulfonate.

2. Reductions by Ti(II) and Ti(III): Overview

Stoichiometric determinations [8], carried out with excess oxidant, confirm that Ti(II) reacts with equimolar quantities of $2e^-$ reagents such as benzoquinones and I_3^-, but with two equivalents of $1e^-$ acceptors such as cobalt(III) complexes and the nitrosodisulfonate anion, $[^\bullet ON(SO_3)_2]^{2-}$

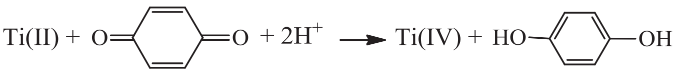
(1)

$$Ti(II) + [I_3]^- \rightarrow Ti(IV) + 3I^- \quad (2)$$

$$Ti(II) + 2Co(III) \rightarrow Ti(IV) + 2Co(II) \quad (3)$$

$$Ti(II) + 2[^\bullet ON(SO_3)_2]^{2-} + 2H^+ \rightarrow 2[HON(SO_3)_2]^- + Ti(IV) \quad (4)$$

Rate laws for reductions, by excess Ti(II), of several cobalt(III) complexes, as well as I_3^- and $[^\bullet ON(SO_3)_2]^{2-}$, are given in Table 1. Corresponding data for Ti(III) are listed, for comparison, in Table 2. Reactions of both $[(NH_3)_5CoCl]^{2+}$ and its fluoro analog, exhibit the straightforward monomial rate law: rate = k[ox][red], with k for the fluoro complex ($630\ M^{-1}\,s^{-1}$) over 10^3-fold greater than that for the chloro ($0.26\ M^{-1}\,s^{-1}$). Reduction of the aqua complex, $[(NH_3)_5Co(H_2O)]^{3+}$ conforms to the inverse-acid rate law (5), indicating a predominant path through the deprotonated ($^{III}Co–OH$) form of the oxidant.

$$\text{rate} = \frac{k[Co^{III}][Ti^{II}]}{[H^+]} \quad (5)$$

Of the nonmetal-derived oxidants, nitrosodisulfonate ($K = 5.3 \times 10^3\ M^{-1}\,s^{-1}$) reacts rapidly without acidity dependence, whereas I_3^- generates the more complex rate law, (6) with both reductants. Note that the constant, K, applies to the formation of I_3^- from I^- and I_2.

$$\text{rate} = \frac{d[I_3^-]}{dt} = \frac{[I_3^-][Ti^{II}](k_0 + k'K[I^-])}{(1 + K[I^-][H^+])} \quad (6)$$

$$I_2 + I^- \rightleftarrows I_3^- \quad (7)$$

$K = [I_3^-]/[I_2][I^-] = (7.0 \pm 0.1) \times 10^2\ M^{-1}$[9]

Unexpectedly, reductions of $[(NH_3)_5CoBr]^{2+}$ and its monoiodo analog with excess Ti(II) yield nearly linear patterns with rates nearly independent of [oxidant] during the first 80–90% of the reaction, before becoming curved. Such profiles are not observed for the corresponding reductions by Ti(III). Moreover, these Ti(II) reductions, but not those by Ti(III), are catalyzed by added Ti(IV). Similar differences appear also when reductions of quinones by Ti(II) and Ti(III) are compared. Mechanistic implications of these contrasts are considered in Section 3.

The question, "Which is the more reactive reductant, Ti(II) or Ti(III)?" is complicated by the plurality of rate laws governing their reactions, and, in part, by the reaction conditions chosen. Table 3 constitutes an attempt, only partially successful, to compare reductions by these states under conditions as similar as possible. Of the eight oxidants included, five, as expected, react more rapidly with Ti(II) than with Ti(III), but in two cases this selectivity is reversed, and there is one instance (the I_3^- reduction) which under the conditions chosen, exhibits a "virtual tie". However, this sampling should not obscure the main point – *that the differences are surprisingly small.*

Estimated formal potentials for Ti(III,II) range from −0.37 V (4) to the much more strongly negative value, −2.1 V [5], whereas that for Ti(III,IV) at pH 0 may be taken as +0.10 V [10]. The difference (>0.47 V) corresponds, in the Marcus treatment for outer-sphere reactions [11], to a rate ratio $k_{Ti(II)}/k_{(Ti(III)} \geq\geq 10^4$.

The much more modest selectives observed in Ti(II)–Ti(III) ratios may imply an unusually low Ti(II,III) self-exchange rate in the media at hand. Both Ti(II) and Ti(III) are, in principle, subject to minor Jahn–Teller distortions, but the extent of each distortion and the occupancy of the non-degenerate orbitals (one short, two long) vs. (two short, one long) may not match. The two states should then have substantially different geometries, and this mismatch would be expected to result in a higher Franck–Condon barrier to exchange. An unusually low self-exchange has been calculated for the analogous d^1, d^2 pair $[V^{IV}O(H_2O)_4]^{2+}$, $[V^{III}(OH)_2(H_2O)_3]^+$ [12].

Rate law (6), which applies to the reduction of tri-iodide by both Ti(II) and Ti(III), is consistent with parallel paths involving I_2 (rate constant k_o) and I_3^- (rate constant k'). Both routes use only the deprotonated reductant, $[Ti^{III}(OH)]^{2+}$ and $[Ti^{II}(OH)]^+$. Concentrations of the two oxidizing species are regulated by the familiar mobile equilibrium (7) ($K_{25^\circ} = 710\ M^{-1}$) [9]. As expected, I_2 is the more rapid oxidizer in both couples, for attachment of I^- to I_2 must disfavor the acceptance of the incoming electron. Superimposed on the parallelism between the rate laws, we see that the contributing parameters for the two systems are remarkably similar.

Comparison of redox rates within the often cited halogenated homologous series, $[(NH_3)_5CoX]^{2+}$ ($X = F^-$, Cl^-, Br^-, and I^-) are complicated by the mechanistic change that intrudes in the Ti(II) reactions of the bromo and iodo oxidants. Nevertheless, it is clear that with both Ti(II) and Ti(III), the fluoro oxidant is by far, the most rapidly reduced and that the reactivity decreases with the heavier members. The trend thus resembles that observed with reductions by Eu(II) [13] and (U(III) [14] but is the reverse of that prevailing in reactions of Cr(II) [15], Fe(II) [16], and In(I) [17]. The implication here is that reactivities of Ti(II) and $[Ti^{III}(OH)]^{2+}$ are governed by the degree of conversion to a fluoro-bound precursor complex [18,19] (e.g. $Ti^{II}–F–Co^{III}$), and that both titanium centers are hard acids in the Pearson sense [16].

Despite evidence for fluoro bridging in $Co^{III}–Ti^{II}$ redox systems, this reductant utilizes inner-sphere paths much less usually than the more versatile donors, Cr^{2+} [15], and In^+ [17].

Rate laws and kinetic parameters for reductions of Fe(III) species by Ti(II) and Ti(III) [20] are compared in Table 4. These reactions are nearly insensitive to added halide and Ti(IV).

In contrast, the reactions of Ru(III) are accelerated by added Ti(IV), with the Ti(IV) dependence exhibiting kinetic saturation at high concentrations of this state. At [Ti(IV)] well below the saturation region, rates are proportional to expression (8)

$$\text{rate} = kK_{cat}[Ru^{II}][Ti^{II}][Ti^{IV}], \quad (8)$$

where K_{cat} pertains to the formation of a 1:1 Ti(II)–Ti(IV) reactive complex obtained by measurements of rates at varying Ti(IV) con-

Table 2
Rate laws and kinetic parameters for oxidations of Ti^{III}(aq).[a]

Ox	Rate law	Parameters
$[NDS^{\bullet}]^{2-}$[b]	$k\,[NDS^{\bullet}][Ti^{III}]$	$k = 1.9 \times 10^3\ M^{-1}\ s^{-1}$
Bzqn[c]	$[Bzqn][Ti^{III}]\ (k_o + k'/[H^+]$	$k_o = 103\ M^{-1}\ s^{-1}$; $k' = 24\ s^{-1}$
CHBzqn[d]	$k[CHBzqn][Ti^{III}]/[H^+]$	$k = 3.3 \times 10^3\ s^{-1}$
$[CoA_5F]^{2+}$[e]	$[Co^{III}][Ti^{III}](k_o + k'/[H^+])$	$k_o = 44\ M^{-1}\ s^{-1}$; $k' = 15\ s^{-1}$
$[CoA_5Cl]^{2+}$[e]	$[Co^{III}][Ti^{III}]k/(K_A + [H^+])$	$k = 1.9 \times 10^{-3}\ s^{-1}$; $K_A = 2 \times 10^{-3}$ M
$[CoA_5Br]^{2+}$[e]	$[Co^{III}][Ti^{III}]k/(K_A + [H^+])$	$k = 1.3 \times 10^{-3}\ s^{-1}$; $K_A = 2 \times 10^{-3}$ M
$[CoA_5I]^{2+}$[e]	$[Co^{III}][Ti^{III}][k_o + k'/[H^+]$	$k_o = 1.4\ M^{-1}\ s^{-1}$; $k' = 0.26\ s^{-1}$
$[CoA_5(H_2O)]^{3+}$[e]	$[Co^{III}][Ti^{III}](k/(K_A + [H^+])$	$k = 2.5 \times 10^{-4}\ s^{-1}$; $K_A = 2 \times 10^{-3}$ M
$[Co(C_2O_4)_3]^{3-}$[f]	$[Co^{III}][Ti^{III}]k_o + k'/[H^+]$	$k_o = 1.5 \times 10^2\ M^{-1}\ s^{-1}$; $k' = 56\ s^{-1}$
I_3^-	$[I_3^-][Ti^{III}](k_o + k'K[I^-])/[H^+](1 + K[I^-])$	$k_o = 2.1\ s^{-1}$; $k' = 0.1\ s^{-1}$; $K = 7 \times 10^2\ M^{-1}$

[a] Reactions at 22 °C; $\mu = 0.5$ M; $[H^+] = 0.1 = 0.5$ M.
[b] Nitrosodisulfonate.
[c] Bzqn = 1.4-Benzoquinone.
[d] 2,5-Dichloro-3,6-dihydroxybenzoquinone.
[e] $CoA_5 = (NH_3)_5Co^{3+}$.
[f] Ref. [24].

Table 3
Rate comparisons for reductions by Ti(II) and Ti(III).[a]

Ox	Medium	$k_{Ti(II)}$[b]	$k_{Ti(III)}$[b]
$[NDS^-]^{2-}$	$[H^+] = 1.0$ M; $\mu = 1.0$ M (HCl/CF_3SO_3H)	5.3×10^3	1.29×10^3
I_3^-	$[H^+] = 0.50$ M; $[I^-] = 0.10$ M; $\mu = 1.0$ M ($HCl/LiCl/CF_3SO_3H$)	0.32	0.35
Bzqn[c]	$[H^+] = 0.50$ M; $\mu = 0.50$ M ($HClO_4$)	2.2×10^2	1.4×10^2
CHBzqn[d]	$[H^+] = 0.50$ M; $\mu = 0.50$ M ($HClO_4$)	6×10^2	6×10^3
$CoA_5(H_2O)^{3+}$[e]	$[H^+] = 0.20$ M; $\mu = 0.50$ M ($HClO_4/NaClO_4/CF_3SO_3H$)	0.16	1.2×10^{-3}[f]
CoA_5F^{2+}	$[H^+] = 0.50$ M; $\mu = 0.50$ M $HClO_4$	6.3×10^2	1.4×10^2[f]
CoA_5Cl^{2+}	$[H^+] = 0.20$ M; $\mu = 0.50$ M ($HClO_4/NaClO_4/CF_3SO_3H$	0.26	1.1×10^{-2}[f]
$Co(C_2O_4)_3{}^{3-}$	$[H^+] = 0.50$ M; $\mu = 0.60$ M ($HCl/NaCl/CF_3SO_3H$)	78[g]	250[g]

[a] Reactions carried out at 22 °C unless otherwise indicated.
[b] Rate constants in $M^{-1}\ s^{-1}$.
[c] 1,4-Benzoquinone.
[d] 2,5-Dichloro-3,5-dihydroxybenzoquinone (II).
[e] $CoA_5 = (NH_3)_5Co^{(III)}$.
[f] 25 °C; $\mu = 0.50$ M (LiCl) Ref. [24].
[g] Ref. [8].

Table 4
Reductions of iron(III) complexes with Ti(II) and Ti(III): rate constants.[a]

Oxidant	$k_{Ti(II)}$ ($M^{-1}\ s^{-1}$)	$k_{Ti(III)}$ ($M^{-1}\ s^{-1}$)
$[Fe(H_2O)_6]^{3+}$	4.2×10^2	1.7×10^2
$[Fe(EDTA)]^+$	4.9×10^3	3.2×10^4
$[Fe(CN)_6]^{3-}$	$5.9 \times 10^4 + 9 \times 10^4\ [H^+]$	1.7×10^5
$[Fe(o\text{-}phen)_3I^{3+}$	$>1.5 \times 10^6$	2.6×10^5

[a] Reactions at 22.5 °C; $\mu = 0.50$ M ($CF_3SO_3H + CF_3SO_3Na$).

Table 5
Reductions of substituted pyridine derivatives of $(NH_3)_5$Ru(III). Kinetic parameters [20].[a]

Oxidant, $[Ru(NH_3)_5(Lig)]^{3+}$	$10^{-4}k$ ($M^{-1}\ s^{-1}$)	K_{eq}[b]
Lig = 4-benzoylpyridine	3.1	104
Lig = 4-pyridinecarboxamide	2.4	118
Lig = 4-acetylpyridine	3.1	100
Lig = 3-acetylpyridine	2.4	102
Lig = pyridine	0.4	114

[a] Reactions at 22.5 °C, $\mu = 0.50$ M ($CF_3SO_3H + CF_3SO_3Na$).
[b] Formation constants for Ti(II)/Ti(IV) intermediate.

centrations [20]. Table 5 compares rates for reductions of Ru(III) derivatives of ring-substituted pyridines.

Neither the Fe(III)–Ti(II) data (Table 4) nor the Ru(III)–Ti(II) data (Table 5) yield evidence for inner-sphere paths. The very rapid Fe(III) oxidants, $Fe(EDTA)^-$, $Fe(CN)_6{}^{3-}$, and $[Fe(o\text{-}phen)_3]^{3+}$ are substitution-inert, and the fastest of this trio, the phenanthroline derivative $k > 10^6\ M^{-1}\ s^{-1}$) is devoid of bridging ligands. Its high reactivity may be reasonably attributed to a combination of its very positive potential (+1.14 V) and the relatively low Franck–Condon barrier associated with passage of an electron to a highly conjugated system.

Rate constants (k values) for the Ru(III)–Ti(II) series (Table 5) show only modest increases arising from substituting keto groups or the $-CONH_2$ function on the ligating pyridine ring, effects comparable to those reported for corresponding reductions by Ti(III) [21], and many orders of magnitude less marked than those increases (five to seven powers of 10), observed for the analogous Co(III)–Cr(II) and Co(III)–Eu(II) series [22]. The very large accelerations in the Co(III) systems are now taken as evidence of electron transfer via preliminary reduction of carbonyl-bearing substituents. With Ti(II), however, we see only minor enhancements, reflecting slight withdrawal from the Ru(III) center.

3. Catalysis by Ti(IV)

Dissimilarities between the redox behavior of Ti(II) and Ti(III) are particularly marked with respect to the homologous oxidant series, fluoro-, chloro-, bromo, and iodo-pentamminecobalt(III). Reductions by Ti(III) yields the expected exponential profiles throughout the series, as were those for the Ti(II)-fluoro and Ti(II)-

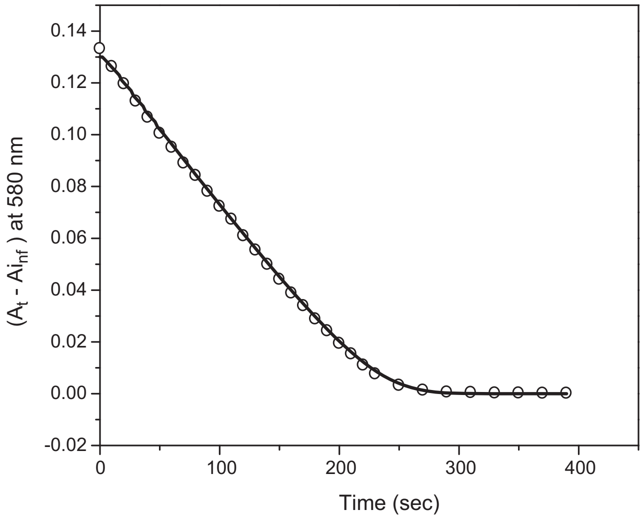

Fig. 1. Kinetic profile for the reduction of $[Co(NH_3)_5I]^{2+}$ with $Ti(II)_{aq}$ (12.0 mM) in the presence of added Ti(IV) (72 mM); $H^+ = 0.7$ M ($CF_3SO_3H/HClO_4$); $\mu = 1.0$ M. Circles represent the experimental data, whereas the solid line was obtained by KINSIM simulation of the proposed mechanism (10) and (11) using parameters $k_1 = 9.5 \times 10^{-3}\ M^{-1}\ s^{-1}$, $k_2/k_{-1} = 22$. Optical path length = 1.00 cm.

chloro systems. Curves for the Ti(II)-bromo and the Ti(II)-iodo reactions are, however, clearly biphasic, featuring a prominent linear (zero-order) component and a small curved portion in the late stages (Fig. 1). No other Co(III) complex mimics the bromo- and iodo-reduction pattern.

In addition, rates in the linear portions of the Ti(II)-bromo the Ti(II)-iodo curves are proportional to the concentration of added Ti(IV), but this catalysis does not extend to the chloro- or fluoro curves, nor to any of the Ti(III) reductions. Initial bromo and iodo rates conform to (9):

$$\text{rate} = -d[Co^{III}]/dt = k[Ti(II)][Ti(IV)][Co(III)]^{o} \quad (9)$$

The biphasic profiles observed, in conjunction with the dependence on [Ti(IV)], are consistent with sequence (10) and (11) for the bromo- and iodo-substituted Co(III) oxidants.

$$[Ti^{II}(H_2O)6]^{2+} + [TI^{IV}F_6]^{2-} \underset{k_{-1}}{\overset{k_1}{\rightleftarrows}} [Ti^{II}(H_2O)5]^{2+} + [(H_2O)Ti^{IV}F_5]^{-} + F^{-} \quad (10)$$

$$[Ti(II)(H_2O)_5]^{2+} + Co(III) \xrightarrow{k_2} Ti(III) + Co(II) \quad (11)$$

Here the active reducing species is taken as the coordinatively unsaturated Ti(II) center, probably $[Ti(H_2O)_5]^{2+}$. Incorporation of sequence (10) and (11) into a KINSIM-related treatment [23] produced calculated absorbance curves which, when compared to the observed kinetic profiles, yielded values for k_1 ($1.0 \times 10^{-2}\ M^{-1}\ s^{-1}$) and the ratios k_2/k_1 (2.0×10^2, bromo; 3.0×10 iodo). Note that treatment does not yield individual values of k_{-1} and k_2 but only their ratios.

An alternative sequence features initiation by a Ti(IV)–Ti(II) comproportionation Ti(II) + Ti(IV) → 2Ti(III)), proceeding electron transfer from Ti(III) to Co(III). Although this is also consistent with the observed biphasic profiles, it is ruled out by the very slow Ti(III) reductions of both the bromo an iodo complexes [24]. More complicated formulations involving transient bi- or polynuclear titanium species analogous to those described by Mattes [25], generate poorer fits.

Since the zero order disappearance of these Co(III) oxidants is ascribed to a preliminary rate-determining transfer of a Ti(II)-bound aqua ligand to an electrophilic Ti(IV) species, we may ask why this heterolysis (which requires no appreciable alteration of the crystal field stabilization energy) is so slow. In the absence of further evidence, it is reasonable to suspect that this sluggishness simply reflects the relative reluctance of the fluorophilic Ti(IV) center to take on an additional (softer and O-donor) ligand.

Catalytic action by Ti(IV) is observed also in the Ti(II) reductions of quinones and oxo species derived from hypervalent metals. [26] Rate laws for various reactions of this type appear in Table 6. All but one of the 1,4-quinones exhibit a $[Ti^{IV}]$-dependence which includes a quotient of type (12) (kinetic saturation) consistent with the formation of a complex of Ti(IV) (association constant K) and a limiting specific rate, k. Refinements of data pertaining to rate

$$\frac{kK[Ti^{IV}]}{1 + K[Ti^{IV}]} \quad (12)$$

laws including quotient (12) lead to the same formation constant ($K = 4 \times 10^2\ M^{-1}$) for this complex, indicating that we are dealing with the same adduct in each system and that Ti(IV) has become attached to the Ti(II) center rather than to each of the various oxidants. The persistence of (12) in the rate laws for the two dihydroxyquinones suggests that the active Ti(II)–Ti(IV) species attacks both the uncharged quinone and its monodeprotonated form, whereas its appearance in both the halide-free and halide-proportional terms in the Mn(IV) reduction (chelate I) indicate that it is involved in both the chloride- and fluoride-catalyzed components, as well as in the halide-free path.

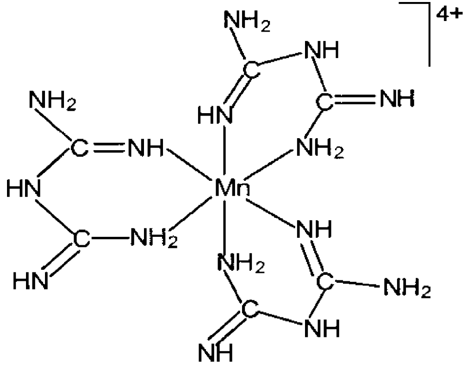

I

Two of the oxidants in Table 6 are consumed without catalysis by Ti(IV). The 1,2-dicarbonyl function of 1,2-naphthoquinone (II) allows a two sided approach to the Ti(II) coreagent (II), and the combined action of the two electron withdrawing sites may disfavor attachment of the Ti(V) center. The very rapid reduction of VO_2^+ may reflect, at least in part, the high formal potential (+1.00 V) of this oxidant and, in addition, the possibility that reaction may occur via oxo transfer. More recent studies of the Ti(II) reductions of the high potential

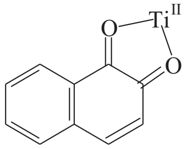

II

metal-oxo species, UO_2^{2+} and MnO_4^- [27], which proceed without Ti(IV)-catalysis, are in accord with this view.

The mechanistic picture applying to Ti(IV)-catalyzed Ti(II)-quinone reactions is complicated by the capacity of both oxidants and reductants to undergo both one- and two-electron changes. Furthermore, if single electron paths are preferred, is an outer-sphere or bridged path utilized? The pervasiveness of Ti(IV) catalysis leads us to favor initiation of single-electron transfer from Ti(II). Since these systems present no spectroscopic evidence for the

Table 6
Catalyzed reductions by titanium(II): rate laws and kinetic parameters.[a]

Oxidant	Rate laws	Parameters
1,4-Benzoquinone	$k_0 = \frac{kK[\mathrm{Ti^{II}}][\mathrm{Ti^{IV}}]}{1+K[\mathrm{Ti^{IV}}]}$	$k = 1.06 \times 10^3$ M^{-1} s^{-1} $K = 4.1 \times 10^2$ M^{-1}
Tetrahydroxy-1,4-benzoquinone	$k_o = \frac{kK[Ti^{II}][Ti^{IV}]}{1+K[Ti^{IV}]}$	$k = 70$ M^{-1} s^{-1} $K = 4.0 \times 10^2$ $M^{-1} = 70$ M^{-1} s^{-1}
2,5-Dichloro-3,6-dihydroxybenzoquinone	$k_o = \left(k_1 + k_2[H^+]^{-1}\right) \frac{K[Ti^{II}][Ti^{IV}]}{1+K[Ti^{IV}]}$	$k_1 = 8.8 \times 10^2$ M^{-1} s^{-1} $k_2 = 35$ s^{-1} $K = 3.7 \times 10^2$ M^{-1}
2,5-Dihydroxy-1,4-benzoquinone	$k_o = \left(k_1 + k_2[H^+]^{-1}\right) \frac{K[Ti^{II}][Ti^{IV}]}{1+K[Ti^{IV}]}$	$k_1 = 4.6 \times 10^2$ M^{-1} s^{-1} $k_2 = 58$ s^{-1} $K = 3.5 \times 10^2$ M^{-1}
1,2-Naphthoquinone	$k_o = k[\mathrm{Ti^{II}}]$	$k = 2.4 \times 10^2$ M^{-1} s^{-1}
Nitrosodisulfonate[b]	$k_o = k[\mathrm{Ti^{II}}][\mathrm{Ti^{IV}}]$	$k = 3.0 \times 10^5$ M^{-2} s^{-1}
$[VO_2]^+$	$k_o = k[\mathrm{Ti^{II}}]$	$k = 9.6 \times 10^3$ M^{-1} s^{-1}
$[Mn^{IV}(bigh)_3]^{4+}$	$k_o = (k_1 + k_2[Hal^-]^{-1}) \frac{K[Ti^{II}][Ti^{IV}]}{1+K[Ti_{IV}]}$	$k_1 = 1.1 \times 10^4$ M^{-1} s^{-1} $K = 3.5 \times 10^2$ M^{-1} $k_2 = 5.0 \times 10^6$ M^{-1} s^{-1} (Hal = F) 1.9×10^6 M^{-1} s^{-1} (Hal = Cl)

[a] Reactions at 22.0 ± 0.5 °C; $\mu = 0.5$ M ($HClO_4$–$NaClO_4$–CF_3SO_3H).
[b] Reactions in LiCl–HCl–CF_3SO_3H.

accumulation of an odd-electron intermediate in any of the quinone reactions, further reaction of the semiquinone intermediate must be rapid and hence kinetically silent.

The proposed sequence for the Ti(IV)-catalyzed quinone reductions is Eqn. (13)–(15):

$$Ti(II) \quad + \quad Ti(IV) \overset{K}{\rightleftarrows} \quad Ti(II) : Ti(IV)(aq) \tag{13}$$

$$\mathrm{Ti(II) : Ti(IV)(aq)} + \underset{\text{quinone}}{\mathrm{O = Q = O}} \rightarrow \underset{\text{semiquinone}}{\mathrm{O = Q = OH}} + \mathrm{Ti(III) : Ti(IV) - OH} \tag{14}$$

$$\mathrm{O = Q - OH + Ti(II) : Ti(IV)(aq)} \rightarrow \underset{\text{hydroquinone}}{\mathrm{HO - Q - OH}} + \mathrm{Ti(III)} : \mathrm{Ti(IV) - OH(rapid)} \tag{15}$$

For those systems exhibiting an inverse$[H^+]$ term in the rate law, this sequence must be supplemented by an analogous route, probably featuring Ti(IV) in its deprotonated form.

Does the suggested electron transfer step, (14), require a preliminary Ti(II)-oxo ridge? Such a bridge should be favored by 2-hydroxy substituents allowing chelation at the reducing center, which would then be expected to enhance reaction rates. However, the several 2-hydroxy-substituted oxidants (Table 6) exhibit rate constants very similar to that for benzoquinone itself (which offers no chelation paths) indicating that the rate-determining steps in the catalyzed conversions are $1e^-$ outer-sphere acts.

4. Molybdenum and copper catalysis [28]

The torpid progress of many reductions by Ti(II), coupled with the pervasive catalysis by Ti(IV), prompts the question, “Are other metal species catalytically effective?” Among those transition metal centers examined, Cu^{2+} and $[MoO_4]^{2-}$ exhibit substantial catalysis, whereas Cr^{3+}, Mn^{2+}, Co^{2+}, Ni^{2+}, and $[WO_4]^{2-}$, under comparable conditions, are without measurable effect.

Kinetic studies of the catalyzed reductions of the oxidants VO^{2+}, benzoquinone, and I_3^-, using excess Ti(II), generate the straightforward binomial rate law (16)

$$\text{rate} = \frac{-\mathrm{d[Ox]}}{\mathrm{d}t} = [\mathrm{Red}][\mathrm{Ox}](k_o + k_{cat}[\mathrm{cat}]) \tag{16}$$

where k_o and k_{cat} denote rate constants for the uncatalyzed and catalyzed components. Note that catalysis by Cu^{2+} was observed only for the VO^{2+}–Ti(II) system. Solutions containing pentapositive molybdenum in its dimeric form, $[Mo_2O_4]^{2+}$ [29], are devoid of catalytic action.

Rate constants obtained from refinements in terms of rate law (16) are summarized in Table 7, along with the corresponding parameters for catalyzed reductions by Ti(III).

Each of the catalyzed paths (Table 7) is first order in catalyst, suggesting that each is initiated by reduction of Mo(VI) to a more reactive lower oxidation state. The latter cannot be the dimeric cation, $[Mo_2O_4]^{2+}$, which persists in these media in the absence of O_2 [30], for this is devoid of catalytic activity. A more likely transient is the metastable monomeric Mo(V) species proposed by Sykes [31], and generated by Chalipoyil and Anson [32]. This monomer

Table 7
Reductions by Ti(II) and Ti(III) as catalyzed by Mo(VI) and Cu(II); kinetic parameters[a] rate = $-\mathrm{d[Ox]}/\mathrm{d}t$ = [Red][Ox] ($k_o + k_{cat}$[cat]).

Ox	Red	Cat	k_o (M^{-1} s^{-1})	k_{cat} (M^{-2} s^{-1})
VO^{2+}	Ti(III)	Mo(VI)	1.70	2.3×10^4
	Ti(III)	Cu(II)	No catalysis	
VO^{2+}	Ti(II)	Mo(VI)	3.3	9×10^3
		Cu(II)	3.1	9×10^3
Bzqn	Ti(II)	Mo(VI)	2.2×10^2	5×10^7
I_3^-[d]	Ti(III)	Mo(VI)	0.33	1.5×10^6
	Ti(II)	Mo(VI)	0.32	7×10^5

[a] Reactions at 22.0 ± 0.5 °C, $\mu = 0.50$ M.
[b] HCl/LiCl.
[c] 0.5 M CF_3SO_3H.
[d] Since the equilibrium involving I_3^- and I_2 is strongly dependent on added iodide, runs with this system were carried out with $[I^-]$ constant at 0.050 M, thus holding the ratio $[I_3^-]/[I_2]$ at 35, [9]. Under these conditions, I_3^- rates closely followed expression (16).

is observable in 10 M HCl but decomposes quickly in 2 M CF_3SO_3H [33].

A reasonable sequence, indicated for the catalyzed Ti(II)-benzoquione reaction is (17)–(19):

$$Ti(II) + Mo(VI) \underset{k_{-1}}{\overset{k_1}{\rightleftarrows}} Ti(III) + Mo(V) \tag{17}$$

$$Bzqn + Mo(V) \xrightarrow{k_2} Mo(VI) + [Bzqn\bullet] \tag{18}$$

$$\mathrm{Bzqn}\bullet + \mathrm{Ti(II)} \xrightarrow{2H^+} \mathrm{Ti(III)} +$$

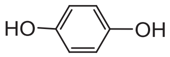

(rapid)

(19)

If the steady state approximation is applied to monomeric Mo(V) under our conditions, and if the reduction of the semiquinone radical is taken to be kinetically silent, the overall rate constant (k_{cat}) approaches k_1k_2/k_{-1}. Rate constants for the individual steps cannot be evaluated from the experiments at hand.

For the Mo(VI)-catalyzed Ti(II)–I_3^- reactions steps (18) and (19) may be replaced by (20) and (21),

$$I_3^- + Mo(V) \rightarrow Mo(VI) + I^{\bullet} + 2I^- \tag{20}$$

$$I^{\bullet} + Ti(II) \rightarrow Ti(III) + I^- \quad (rapid) \tag{21}$$

and the catalyzed VO^{2+}–Ti(II) reaction may be taken to utilize propagation via (22)

$$V(IV) + Mo(V) \rightarrow V(III) + Mo(VI) \tag{22}$$

An analogous sequence is reasonable for the catalyzed Ti(III)–I_3^- reaction, but in this instance initiation would be expected to proceed via (23)

$$Ti(III) + Mo(VI) \rightarrow Ti(IV) + Mo(V) \tag{23}$$

Reversal of initiation step (23) appears to be negligible, for the overall reaction is not inhibited by addition of Ti(IV) at concentrations as high as 0.60 mM.

Catalysis by Cu(II) may be taken to be initiated by reaction (24),

$$Ti(II) + Cu(II) \rightarrow Ti(III) + Cu(I) \tag{24}$$

in analogy with (17) which applies to Mo(VI) catalysis. Rate constants pertaining to the catalytic components (k_{cat} values) for the VO^{2+}–Ti(II) reactions, as catalyzed by Cu(II) and by Mo(VI) are remarkably similar, but this resemblance appears to be coincidental rather than mechanistically significant. Note that the catalytic constant associated with the Ti(II)–I_3^- reaction (7×10^5 M^{-2} s^{-1}) is less than that for Ti(III) (1.5×10^6 M^{-2} s^{-1}), but the difference is slight and calls to mind differences pertaining to uncatalyzed reactions of these states (Section 2).

5. Reductions of molybdenum(VI) [34]

Catalysis by Mo(VI) reductions by Ti(II) and Ti(III) generates a different mechanistic picture from that pertaining to the more familiar catalytic use of H_2MoO_4 in accelerating oxygen atom transfer from peroxy compounds to alkenes and amines. The latter oxygenations are most often considered to involve complexes of Mo(VI) with the oxidants [35], whereas the titanium reactions at hand require reduction of the molybdenum center. However, the dimeric cation, $[Mo_2O_4]^{2+}$, a persistent form of Mo in the pentapositive state in aqueous triflate, is catalytically inactive for Ti(II) and Ti(III) systems.

Quantitative reduction of Mo(VI) to the stable green Mo(V) complex, $[MoOCl_5]^{2-}$, may be carried out in 11.0 M HCl using Ti(II), Ti(III), V(II), or Ge(II) [34], but such reactions monitored at 430 nm in triflate medium generate more informative profiles. In each case, a marked increase in absorbance, followed by a sharp drop, is evident (e.g., Fig. 2). Peak absorbance generally occurs during the first second after mixing. Treatment of these profiles as consecutive first order processes (25) allows separation of the rate constants (k_1 and k_2) and calculation of the molar absorbances of the intermediates [36].

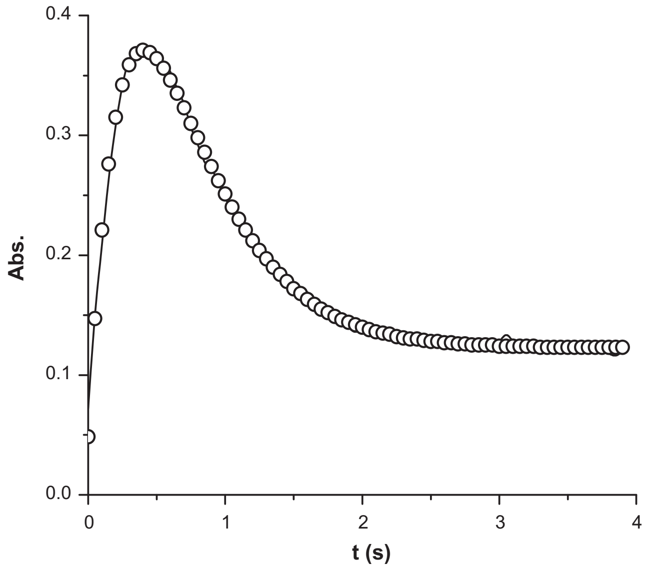

Fig. 2. Kinetic profile for the reaction of H_2MoO_4 (0.30 mM) with V(II) (12 mM); $[H^+]$ = 0.50 M, λ = 430 nm. The solid line represents the experimental curve; the circles were calculated by refinement, using the relationship of Bose [36]; kinetic parameters in Table 9.

$$Mo(VI) + Red \xrightarrow{k_1} \text{intermediate} \xrightarrow{k_2} products \tag{25}$$

Rate laws for formation of the intermediate by V(II) and by Ge(II), included here for comparisons, are straightforward monomial expressions:

$$\text{rate} = k[\text{Mo(IV)}][\text{Red}] \qquad k_{V(II)} = 2.3 \times 10^2\ M^{-1}\ s^{-1} \tag{26}$$

$$k_{Ge(II)} = 9.4 \times 10^2\ M^{-1}\ s^{-1} \tag{27}$$

In contrast, reductions by Ti(II) and Ti(III) are inhibited by H^+ (28) and also by Cl^- (29), leading to rate laws and parameters listed in Table 8.

The array of biphasic profiles is consistent with the view that Mo(VI) reacts quickly in acid solutions with each of the metal-center reductants, yielding an intermediate which strongly absorbs at 430 nm, and which decays ultimately to the familiar cation, $[Mo_2O_4]^{2+}$. The properties of this transient correspond to those of the monomeric Mo(V) species described by Anson [32]. This monomer is converted to a more stable chloro complex in 10 M HCl, but decomposes quickly in 2 M CF_3SO_3H and is most probably involved also in the Mo(VI)-catalyzed reductions of benzoquinone, vanadium(IV), and tri-iodide by hypovalent titanium (Section 4).

Although the generation of Mo(V) by both V(II) and Ge(II) proceeds according to simple monomial rate laws (36), both conversions pose mechanistic questions. The Mo(VI)–Ge(II) reaction may avoid the unstable state Ge(II) by preliminary formation of Mo(IV), probably by oxo transfer (31), followed by rapid Mo(IV)–(VI) comproportionation (31).

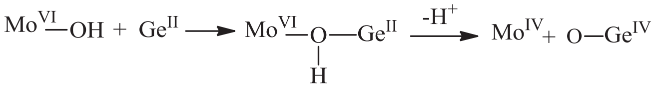

$$Mo^{VI}{-}OH + Ge^{II} \longrightarrow Mo^{VI}{-}\underset{\displaystyle H}{\underset{|}{O}}{-}Ge^{II} \xrightarrow{-H^+} Mo^{IV} + O{-}Ge^{IV} \tag{30}$$

Table 8
Reductions of Mo(VI); generation of Mo(V) intermediate. Rate laws and kinetic parameters.[a]

Red.	Medium	Rate laws	Parameters
V(II)	CF_3SO_3H/CF_3SO_3Na	$k[\mathrm{Mo(VI)}][\mathrm{V(II)}]$	$k = 2\times10^2\ \mathrm{M^{-1}\,s^{-1}}$
Ge(II)	HCl/LiCl	$k[\mathrm{Mo(VI)}][\mathrm{Ge(II)}]$	$k = 9\times10^2\ \mathrm{M^{-1}\,s^{-1}}$
Ti(II)	CF_3SO_3H/CF_3SO_3Na	$\frac{[Mo(VI)][Ti(II)kK_A}{K_A+[H^+]}$ (28)	$k = 6\times10^3\ \mathrm{M^{-1}\,s^{-1}}$ $K_\mathrm{A} = 0.23\ \mathrm{M}$
Ti(III)	HCl/LiCl	$\frac{[Mo(VI)][Ti(III)]kK_A[H^+]}{(1+K_A[Ti(III)])(1+K_A[H^+]+K_{Cl}[Cl^-])}$ (29)	$k = 150\ \mathrm{M^{-1}\,s^{-1}}$ $K_\mathrm{A} = 0.44\ \mathrm{M}$ $K_\mathrm{Cl} = 0.7\ \mathrm{M^{-1}}$
Eu(II)	HCl/LiCl		$k > 1\times10^4\ \mathrm{M^{-1}\,s^{-1}}$[b]

[a] Reactions at 22 °C, $\mu = 0.50$ M, $\lambda = 430$ nm.
[b] Lower limit.

Table 9
Reductions of Mo(VI); decomposition of Mo(V) intermediate. Rate laws and kinetic parameters.[a]

Red.	Medium	Rate laws[b]	Parameters
V(II)	CF_3SO_3H/CF_3SO_3Na	$\frac{kK_A[Int]}{K_A+[H^+]}$	$k = 6\ \mathrm{s^{-1}}$ $K_\mathrm{A} = 0.15\ \mathrm{M}$
Ti(II)	CF_3SO_3H/CF_3SO_3Na	$\frac{kK_A[Int]}{K_A+[H^+]}$	$k = 2.1\ \mathrm{s^{-1}}$ $K_\mathrm{A} = 0.42\ \mathrm{M}$
Ge(II)	HCl/LiCl	$k[\mathrm{Int}]$	$k = 0.41\ \mathrm{s^{-1}}$
Ti(III)	HCl/LiCl	$\frac{k[\mathrm{Ti(III)}][\mathrm{H^+}]\left[\mathrm{Cl^{-1}}\right][\mathrm{Int}]}{1+K_\mathrm{Ti}[\mathrm{Ti(III)}]}$	$k = 9\times10^3\ \mathrm{M^{-3}\,s^{-1}}$ $K_\mathrm{Ti} = 2\times10^2\ \mathrm{M^{-1}}$
Eu(II)	HCl/LiCl	$\frac{(k+k'(\mathrm{Cl^-}])[\mathrm{Int}]}{(1+[H^+]/K_\mathrm{HA}+K_{Cl}[\mathrm{Cl^-}])}$	$k = 60\ \mathrm{M^{-1}\,s^{-1}}$ $K_\mathrm{Cl} = 0.3\ \mathrm{M^{-1}}$ $K_\mathrm{HA} = 0.22\ \mathrm{M}$

[a] Reactions at 22 °C, $\mu = 0.50$ M, $\lambda = 430$ nm.
[b] Rates refer to decomposition of the intermediate, Int, $-d[\mathrm{Int}]/dt$.

$$\mathrm{Mo^{IV} + Mo^{VI} \rightarrow 2Mo^{V}} \qquad (31)$$

The rate constant for the Mo(VI)–V(II) reaction, $2\times10^2\ \mathrm{M^{-1}\,s^{-1}}$, exceeds the 1×10^2 upper limit imposed by slow substitution at the V(II) center [37], thus indicating either a predominant outer-sphere path or an inner-sphere path involving substitution at the Mo(VI) center for this transfer.

The second phase of these profiles, a sharp absorbance decrease (Table 9) is taken to reflect the transformations of the monomeric Mo(V) transient to the inactive dimer, $[\mathrm{Mo_2O_4}]^{2+}$. Two features of these curves are unexpected: (A) The decay portions exhibit no sign of second order character, which one would expect for a monomer-to-dimer conversion, and (B) The calculated molar absorbances of transients generated from the several reductants do not match (Table 10).

It is therefore concluded that the losses of transient are first order processes preceding a rapid, kinetically silent dimerization, and that these transients, although related, are not the same species. Moreover, the rate laws and kinetic parameters associated with the decays are not the same (Table 9).

The kinetic behavior of these intermediates is consistent with the intervention, in at least some cases, of binuclear successor complexes that are formed in the initial electron transfer (33) and which subsequently dissociate to a monomeric Mo(V) species (34) before rapid conversion to the dimeric product (35)

Table 10
Extinction coefficients of Mo(V) intermediate (430 nm).[a]

Red	$10^{-3}\,\varepsilon_\mathrm{Int}$ ($\mathrm{M^{-1}\,cm^{-1}}$)
Ti(II)	1.12 ± 0.11
Ti(III)	1.54 ± 0.28
V(II)	1.50 ± 0.23
Ge(II)	0.84 ± 0.02
Eu(II)	0.33 ± 0.02

[a] ε values obtained from treatment of the biphasic reaction curves using the method of Bose (Ref. [36]).

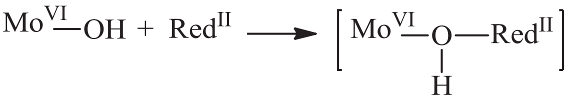
$$\mathrm{Mo^{VI}{-}OH + Red^{II} \longrightarrow \left[Mo^{VI}{-}\underset{\mathrm{H}}{\underset{|}{O}}{-}Red^{II}\right]} \qquad (32)$$

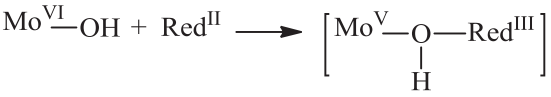
$$\mathrm{Mo^{VI}{-}OH + Red^{II} \longrightarrow \left[Mo^{V}{-}\underset{\mathrm{H}}{\underset{|}{O}}{-}Red^{III}\right]} \qquad (33)$$

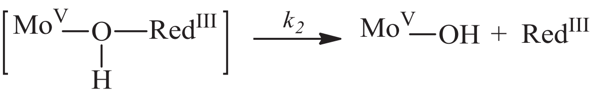
$$\mathrm{\left[Mo^{V}{-}\underset{\mathrm{H}}{\underset{|}{O}}{-}Red^{III}\right] \xrightarrow{k_2} Mo^{V}{-}OH + Red^{III}} \qquad (34)$$

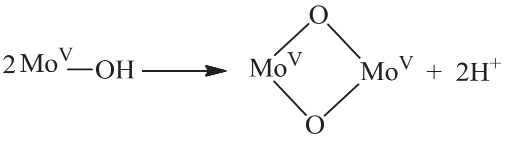
(35)

The various rate laws for decomposition of the Mo(V) transients (Table 9) reflect the speciation of the successor complexes. With both V(II)–V(III) and Ti(II)–Ti(III) systems, dissociation (34) requires deprotonation as indicated by $[\mathrm{H^+}]$ in the denominators, whereas the Ti(III)-Ti(IV) intermediate requires action of additional reductant for dissociation as well as both protonation and $\mathrm{Cl^-}$ attachment. The kinetic saturation with respect to Ti(III) allows the estimation of a stability constant near 200 $\mathrm{M^{-1}}$ for coordination of the additional reductant. The possibility of interaction between Ti(III) and Ti(IV) centers calls to mind the formation of a Ti(III)–Ti(IV) complex in aqueous sulfate as reported by Fraser and co-workers [38].

6. Reactions with hypervalent chromium [39]

The first d-block of transition metals features several members having three or more accessible mononuclear oxidation states separated by single units. When a di- or multivalence change results from reaction with a $2e^-$ coreagent, it may be asked whether the overall transformation involves a series of single electron steps, whether $2e^-$ transfer is at work, or whether a combination of the two modes is operating.

As early as 1948, Watanabe and Westheimer [40] recorded rate experiments which suggested the involvement of the less usual Cr(IV) and Cr(V) states in the reduction of Cr(VI) with 2-propanol, and in 1991, Ghosh and co-workers [41] reported that reductions of $\mathrm{HCrO_4}^-$ with As(III) or Sn(II) in aqueous media buffered by 2-ethyl-2-hydroxybutanoic acid (HLig) and its anion ($\mathrm{Lig^-}$) yielded pink solutions of Cr(IV) chelates of this buffer without major inter-

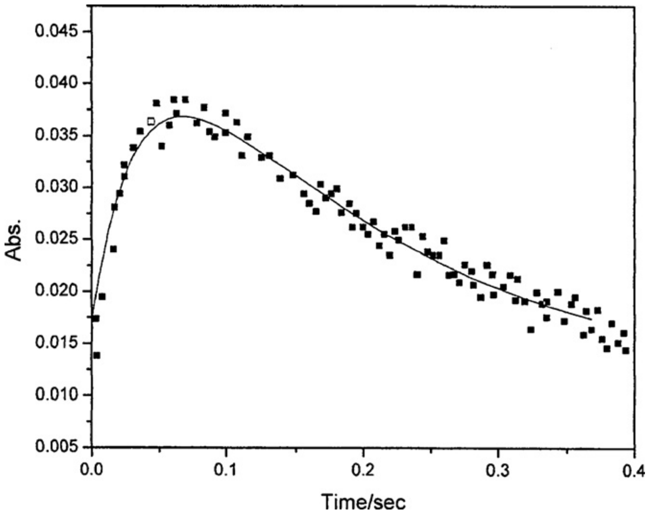

Fig. 3. Kinetic profile of the reaction of Cr(IV) with Ti(II), at 22 °C, monitored at 510 nm. Chelator 2-ethyl-2-hydroxybutanoic acid and its sodium salt added; pH 3.08. Small squares are experimental data, and the solid line was calculated as described by Bose [36], taking contributing rate constants as 8 and 6.2 s^{-1}.

vention of Cr(V).

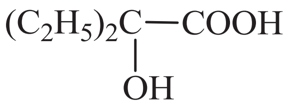

$$(C_2H_5)_2C(OH)-COOH$$

Shortly afterwards, Scott et al. [42] described reactions of a short lived oxidizing species, the behavior of which corresponded to an oxochromium(IV) cation $[Cr^{IV}O]^{2+}$, that reacts with a series of primary and secondary alcohols in two-unit events, bypassing Cr(III). Moreover, Chandra has reported reductions of Cr(VI) to Cr(IV), and thence to Cr(II), using hypophosphite [42] and formate [43], without intervention of Cr(V) or Cr(III).

In contrast, the reactions of hypervalent manganese species featuring Mn(III), Mn(IV), and Mn(III,IV) centers, with the $2e^-$ reductants Sn(II), Ge(II), and In(I) [44] exhibit no transients or kinetic features attributable to $2e^-$ transactions.

Reductions, of Cr(VI), Cr(V),and Cr(IV) using Ti(II), in $HClO_4$–CF_3SO_3H media proceed rapidly and yield Cr(III) in each case

$$2Cr^{VI} + 3Ti^{II} \rightarrow 2Cr^{III} + 3Ti^{IV} \tag{36}$$

$$Cr^{V} + Ti^{II} \rightarrow Cr^{III} + Ti^{IV} \tag{37}$$

$$2Cr^{IV} + Ti^{II} \rightarrow 2Cr^{III} + Ti^{IV} \tag{38}$$

When the Cr(VI)–Ti(II) reaction is carried out in the presence of the chelator 2-ethyl-2-hydroxybutanoate, which is known to stabilize solutions of both Cr(V) and Cr(IV) [45], reaction profiles are diphasic (e.g., Fig. 3), featuring a rapid rise in absorbance, followed by a gradual decay. With Ti(II) in excess, curves are analyzed by treating the system as consecutive pseudo-first order processes (39) then evaluating the contributing rate constants k_1 and k_2 [36]. The k_2

$$Cr(VI) \xrightarrow{Ti^{II},\ k_1} Cr(V) \xrightarrow{Ti^{II},\ k_2} Cr(III) \tag{39}$$

value corresponds to that obtained from Cr(V) independently. Neither of these components involves Cr(IV), which reacts much more rapidly than both Cr(VI) and Cr(V). Rate laws and kinetic parameters for these systems appear in Table 11, which includes values pertaining to reductions by Ti(III) for comparison.

A key question, "Can Ti(II) reduce chromium species using only $2e^-$ transfers?" is addressed by trapping experiments. The trapping reagent is $[Co(NH_3)_5Br]^{2+}$, which reacts very rapidly with Cr^{2+} ($k = 1.4 \times 10^6\ M^{-1}\ s^{-1}$ at 25 °C), but not with other chromium ions. Intervention of Cr(II) should yield Co(II), which may be detected as the deep blue $CoCl_4{}^{2-}$ complex at 692 nm in con HCl.

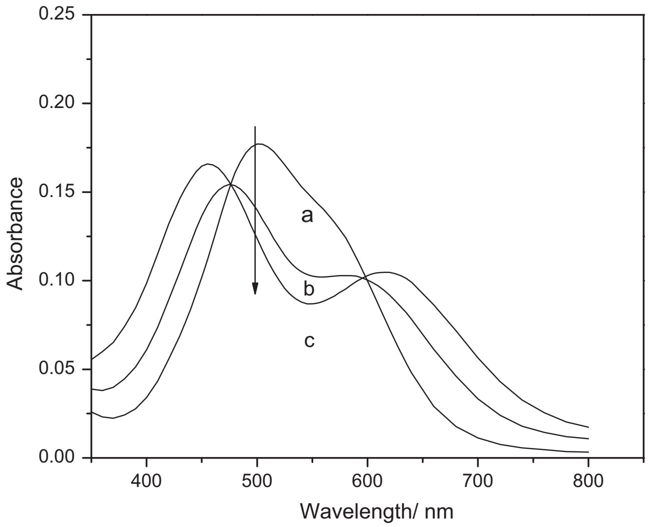

Fig. 4. Conversion of 0.045 M Ti(III) to Ti(II) and Ti(IV) in 0.50 M CF_3SO_3H by addition of HF. Curve *a*, no HF; curve *b*, 0.0375 M HF; curve *c*, 0.0675 M HF. Vertical line denotes the change in absorbance at 500 nm as HF is added.

The trapping studies described establish the absence of $2e^-$ paths for the Ti(II) reductions of Cr(VI) and Cr(IV). A similar conclusion applied to the reduction of Cr(V) is not possible but must be considered very unlikely in view of the earlier demonstrated $1e^-$ paths for its reductions by bisulfite [46], ascorbate [47], and nitrite [48].

Straightforward exponential profiles are obtained for the Cr(VI)–Ti(II) reaction in the absence of chelating ligands which stabilize Cr(V) and Cr(IV). The two-term rate law, (40) points to competing protonated (k_H) and deprotonated (k_o) paths

$$\text{rate} = [Ti^{II}][Cr^{VI}](k_o + k_H[H^+]) \tag{40}$$

and is in accord with a sequence in which rates are determined by an initial step preceding rapid (kinetically silent) acts leading to formation of Cr(III). The site of protonation may be taken to be the Cr(VI)-bound carbonyl function, as has been proposed for other oxidations by Cr(VI) [49].

7. Ti(II)–Ti(III) interconversions in fluoride media [50]

Treatment of pink solutions of Ti(III) in 0.5 M triflic acid with successive portions of HF results in fading of the Ti(III) peak at 500 nm and the growth of peaks at 430 and 650 nm typifying Ti(II) [5]. Isosbestic points appear at 490 and 600 nm (Fig. 4). The reaction is a disproportionation which is favored by the strong affinity of fluoride for Ti(IV) [50].

$$2Ti(II) + 4HF \rightarrow TiF_4 + Ti(II) + 4H^+ \tag{41}$$

For this system, a simplified reaction quotient (50) applies, since $[H^+]$ is kept at 0.5 M, $[F^-]$ is negligible, and [Ti(II)] = [Ti(IV)]. Variation of absorbance at 500 nm with different HF concentrations (Fig. 5) allows calculation of $K_{3.2}$ as $2.4 \times 10^5\ M^{-4}$.

$$K_{3.2} = \frac{[Ti(II)]^2}{[Ti(III)]^2[HF]^4} \tag{42}$$

Similar treatments of data at 430 and 640 nm yield $K_{3.2} = 2.3 \times 10^5\ M^{-4}$. Hence, at the acidity chosen, equimolar concentrations of Ti(II) and Ti(III) coexist in equilibrium in 0.045 M HF, and conversion to Ti(II) is 99% complete in 0.45 M HF.

Table 11
Reductions of hypervalent chromium with Ti(II) and Ti(III). Rate laws and kinetic parameters.

Oxidant	λ (nm)	Rate laws	Parameters
(A) Reductions with Ti(II)			
Cr(VI)[a]	350	$[\mathrm{Cr^{IV}}][\mathrm{Ti^{II}}](k_o + k_H[\mathrm{H^+}])$	$k_o = 2.3 \times 10^3\ \mathrm{M^{-1}\ s^{-1}}$, $k_H = 18.3\ \mathrm{M^{-2}\ s^{-1}}$
Cr(VI)[b]	510	$k_{cat}K[Cr^{VI}]\frac{[Ti^{II}][Ti^{IV}]}{1+K[Ti^{IV}]}$	$k_{cat} = 16 \times 10^4\ \mathrm{M^{-1}\ s^{-1}}$, $K = 2 \times 10^2\ \mathrm{M^{-1}}$
Cr(V)[b,c]	510	$k[\mathrm{Cr^{V}}][\mathrm{Ti^{II}}]$	$k = 6 \times 10^4\ \mathrm{M^{-1}\ s^{-1}}$
Cr(V)[b]	510	$k[\mathrm{Cr^{V}}][\mathrm{Ti^{II}}]$	$k = 5 \times 10^4\ \mathrm{M^{-1}\ s^{-1}}$
Cr(IV)[b]	510	$k[\mathrm{Cr^{IV}}][\mathrm{Ti^{II}}]$	$k = 6 \times 10^5\ \mathrm{M^{-1}\ s^{-1}}$
(B) Reductions with Ti(III)			
Cr(VI)[a]	350	$k[\mathrm{Cr^{IV}}][\mathrm{Ti^{III}}]$	$k = 4 \times 10^3\ \mathrm{M^{-1}\ s^{-1}}$
Cr(VI)[b]	510	$k[\mathrm{Cr^{VI}}][\mathrm{Ti^{III}}]$	$k = 1.0 \times 10^3\ \mathrm{M^{-1}\ s^{-1}}$
Cr(V)[b,d]	510	$[\mathrm{Cr^{V}}][\mathrm{Ti^{III}}](k_o + k_2\ [\mathrm{HLig}])$[f]	$k = 1.2 \times 10^4\ \mathrm{M^{-1}\ s^{-1}}$, $k_2 = 3 \times 10^2\ \mathrm{M^{-2}\ s^{-1}}$
Cr(IV)[e]	510	$k[\mathrm{Cr^{IV}}][\mathrm{Ti^{III}}]$	$k = 1.3 \times 10^5\ \mathrm{M^{-1}\ s^{-1}}$

[a] $[\mathrm{H^+}] = 0.05$–0.50 M ($\mathrm{HClO_4/CF_3SO_3H}$), $\mu = 0.50$ M; no chelating ligand added.
[b] pH 3.08, [HLig] + [NaLig] = 0.28 M.
[c] Lower portion of Cr(VI)–Ti(II) curve.
[d] Ref. [36].
[e] pH 3.50; [HLig] + [NaLig] = 0.01 M.
[f] HLig = 2-ethyl-2-hydroxybutanoic acid.

The Ti(II/III/IV) equilibrium in fluoride media affects the kinetic redox picture in varying degrees. For Ti(III) reductions, with HF absent or very dilute, the usual exponential curves (Section 2) are observed; but for Ti(II) reductions, profiles exhibit prominent zero order character with net rates almost independent of [oxidant] [51]. In Fig. 6, which depicts the curve for the Ti(II)-benzoquinone reaction in 0.5 M $\mathrm{CF_3SO_3H}$ with added HF and Ti(IV), a major portion of the profile is nearly linear. The slope of this portion is proportional to $[\mathrm{Ti^{II}}]$ taken and to $[\mathrm{Ti^{IV}}]$ added. Slight acceleration occurs during the first few percent of reaction, and curvature becomes important during the final stages as the oxidant becomes nearly consumed.

This kinetic behavior, in conjunction with the ease of the Ti(II)/Ti(III) interconversion in fluoride-containing media, points to sequence (43)–(45) for the Ti(II)–quinone reactions

$$Ti(II) \ + \ TiF_4 \ \underset{k_{-1}}{\overset{k_1}{\rightleftarrows}} \ 2 \ Ti(III) \ + \ 4 \ F^- \qquad (43)$$

$$T(III) \ + \ Q \ \xrightarrow{k_2,\ H^+} \ Ti(IV) \ + \ QH\bullet \qquad (44)$$

$$QH\bullet \ + \ Ti(II) \ \xrightarrow{H^+} \ QH_2 \ + \ Ti(III) \quad (rapid) \qquad (45)$$

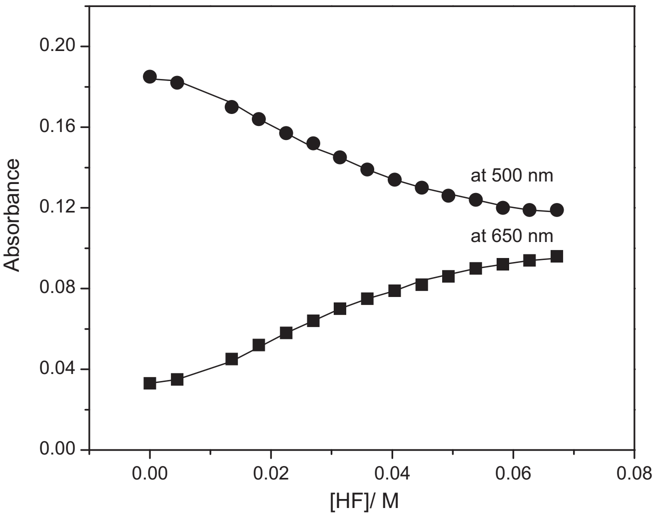

Fig. 5. Observed and calculated absorbance changes at 500 and 650 nm as HF is added to Ti(III). Solid lines are calculated from reaction quotient (50) ($2.6 \times 10^2\ \mathrm{M^{-4}}$). Extinction coefficients (in $\mathrm{M^{-1}\ cm^{-1}}$) were: $\varepsilon_{\mathrm{Ti(III)}}$ 4.10 (500 nm) 0.74 (650 nm) and $\varepsilon_{\mathrm{Ti(II)}}$ 4.50 (500 nm) and 4.9 (650 nm).

Incorporation of sequence (43)–(45) into the KINSIM treatment, [23], yields curves which were compared with the observed profiles. Kinetic parameters giving optimum agreement with the experimental run (Fig. 6) are listed in Table 12, along with parameters obtained from experiments with different oxidants and various reagent concentrations. Parallel treatments of runs at different acidities indicate that k_1 and k_{-1} do not vary significantly with $[\mathrm{H^+}]$, whereas k_2 falls from 150 to 90 $\mathrm{M^{-1}\ s^{-1}}$ between 0.25 and 7.5 mM HF, reflecting the smaller magnitude of the $1/[\mathrm{H^+}]$ contribution at higher acidity (cf. Table 2). As expected, values of k_1 and k_{-1} are independent of the oxidant, which is waiting to enter the picture. The ratio $[\mathrm{Ti^{III}/Ti^{II}}]$ in this medium may be estimated as $(k_1/k_{-1})^{1/2}$ or 5.0. The modest value of this ratio reminds us that in the fluoride-rich preparation the effective oxidation potentials of Ti(II) and Ti(III) approach each other and that this trend stems not from complexation of Ti(II), but rather from ligation of Ti(IV), the co-product from Ti(III).

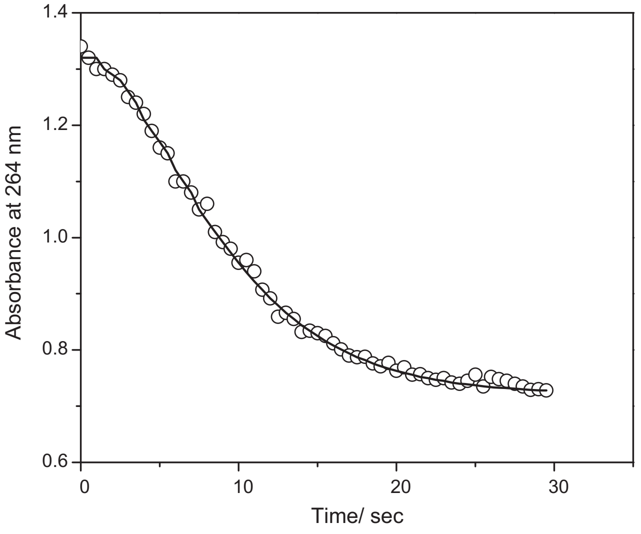

Fig. 6. Kinetic profile at 246 nm for reaction of 1,4-benzoquinone with Ti(II) in 0.50 M $\mathrm{CF_3SO_3H}$, [Ti(IV)] = 1.0 mM, [HF] = 0.35 mM, [quinone] = 0.05 mM. Circles represent experimental data, whereas the solid line was obtained by KINSIM simulation [23] of the proposed mechanism (51)–(53), taking k_1 as 120 $\mathrm{M^{-1}\ s^{-1}}$ and k_2 as 150 $\mathrm{M^{-1}\ s^{-1}}$. Path length = 1.00 cm.

Table 12
Titanium(II) reductions of 1,4-benzoquinones in systems having added HF and added Ti(IV). Kinetic parameters.[a]

Quinone	[HF] (mM)	k_1[b]	k_{-1}[b]	k_2[b]
Chloranilic acid[e]	0.25	110	5.0	2300
	2.5	115	5.0	1400
	5.0	105	3.9	640
	7.5	105	5.0	360
	7.5	110	5.0	370[c]
	7.5	120	5.0	380[d]
1,4-Benzoquinone	0.25	120	5.0	150
	2.5	104	4.0	120
	5.0	110	5.0	95
	7.5	106	4.4	90
Tetrahydroxy-1,4-benzoquinone	0.25	100	5.0	280
	2.5	104	5.0	200
	5.0	110	5.0	180
	7.5	106	4.4	180

$$(51)\ Ti(II) + Ti(IV) \underset{k_{-1}}{\overset{k_1}{\rightleftarrows}} 2\ Ti(III),\ (52)\ Ti(II) + Q \xrightarrow{k_2,\ H^+} Ti(IV) + QH^{\bullet}$$

[a] Component rate constants (22 °C) obtained by KINSIM treatment (Ref. [23]) of kinetic data for Ti(II) reductions of benzoquinones in 0.50 M CF_3SO_3H in the presence of 2.0 mM Ti(IV) and added HF, [Ox] = 0.01 mM; [Ti(II)] = 1.0 mM unless otherwise indicated.

[b] Second order rate constants giving optimal fit of calculated and observed kinetic curves.

[c] [Ti(II)] = 0.25 mM.

[d] [Ti(II)] = 0.50 mM.

[e] 2,5-Dichloro-3,6-dihydroxybenzoquinone.

8. Final remarks

The study of the aqueous chemistry of Ti(II) is in its very early stage. Although a number of novel points have emerged, it is emphasized that virtually all samples examined contain both HF and Ti(IV). Further progress requires the preparation of Ti(II) solutions which are free of such contaminants. Since these species serve to stabilize Ti(II), it is likely that their removal will demand work at lower temperatures and the rapid detection of short-lived transients. Such difficulties, in conjunction with the mobile Ti(II)–Ti(III) equilibria at high fluoride concentrations (Section 7), make it doubtful that Ti(II) solutions will soon replace those of the more robust state Ti(III) as high utility analytical or preparative reductants.

It is instead likely that a more promising future for Ti(II) lies in materials science. Interest in mixed valence solids of a d-block metals has expanded explosively [52], and such systems have achieved prominence as superconductors, pigments, and agents for biological energy transfer and storage.

Reports of titanium-derived mixed valence solids are rare and deal mainly with Ti(III)–Ti(IV) couples [53]. It is anticipated that extension of effort to solid fluoride-based Ti(II)–Ti(III) systems may lead to new facets, in view especially of the ease of interconversion between the two states.

Acknowledgements

I am pleased to acknowledge the contributions of Dr. Z. Yang, B. B. Dhar, and R. Mukherjee, who carried out the work upon which a major portion of this review is based. I am also indebted to the National Science Foundation for partial support of this research. Thanks go also to Dr. Songping Huang and Dr. Yuriy Tolmachev for helpful discussions and to Ms. Arla Dee McPherson and Ms. Erica Lilly for technical assistance.

I am grateful to a reviewer for calling my attention to two interesting recent developments in hypovalent titanium chemistry: (1) “One-Step Direct Synthesis of a Ti-Doped Sodium Alanate Hydrogen Storage Material” [54]; and (2) “The Catalytic Hydroamination of Alkynes” [55].

References

[1] K. Ziegler, E. Holzkamp, H. Breil, H. Martin, Angew. Chem. 67 (1955) 541.
[2] (a) E.A. Minta, in: R.B. King (Ed.), Encyclopedia of Inorganic Chemistry, vol. 8, Wiley, New York, 1994, p. 4206;
(b) S.B. Smith, D.W. Stephan, in: J.A. McCleverty, T.J. Meter (Eds.), Comprehensive Coordination Chemistry, vol. 4, Elsevier, Amsterdam, 2004 (Chapter 4.2).
[3] F. Sato, N. Urabe, in: I. Marek (Ed.), Titanium and Zirconium in Organic Synthesis, Wiley, New York, 2002, p. 281.
[4] (a) C.S. Forbes, L.P. Hall, J. Am. Chem. Soc. 46 (1924) 385;
(b) J.W. Olver, J.W. Ross Jr., J. Am. Chem. Soc. 85 (1963) 2565.
[5] U. Kolle, P. Kolle, Angew. Chem. Int. Eng. 42 (2003) 4540.
[6] Z. Yang, E.S. Gould, Dalton Trans. (2005) 1781.
[7] R.M. Smith, A.E. Martell, Critical Stability Constants, vol. 4, Plenum, New York, 1971, p. 99.
[8] Z. Yang, E.S. Gould, Dalton Trans. 21 (2004) 3601.
[9] D.A. Palmer, R.W. Ramette, R.E. Mesmer, J. Sol. Chem. 13 (1984) 673.
[10] W.J. James, J.W. Johnson, in: A.J. Bard, R. Parsons, J. Jordan (Eds.), Standard Potentials in Aqueous Solution, Marcell Dekker, New York, 1985 (ch. 18).
[11] R.A. Marcus, Annu. Rev. Phys. Chem. 15 (1964) 155.
[12] M.C. Ghosh, E.S. Gould, J. Am. Chem. Soc. 115 (1993) 3167.
[13] J.P. Candlin, J. Halpern, D.L. Trimm, J. Am. Chem. Soc. 86 (1964) 1019.
[14] R.T. Wang, J.H. Espenson, J. Am. Chem. Soc. 93 (1971) 380.
[15] J.P. Candlin, J. Halpern, Inorg. Chem. 4 (1965) 766.
[16] F. Basolo, R.G. Pearson, Mechanisms of Inorganic Reactions, 2nd edn., Wiley, New York, 1968 (Chaps. 1 and 6, Tables 1-9 and 6-4).
[17] S.K. Chandra, E.S. Gould, Inorg. Chem. 35 (1996) 3159.
[18] A. Haim, Inorg. Chem. 7 (1968) 1475.
[19] A.G. Lappin, Redox Mechanisms in Inorganic Chemistry, Ellis Harwood, New York, 1994 (See, for example ch. 5).
[20] R. Mukherjee, V. Manivannan, E.S. Gould, Inorg. Chim. Acta 360 (2007) 3633.
[21] S.K. Chandra, P.C. Paul, E.S. Gould, Inorg. Chem. 36 (1997) 4684.
[22] E.S. Gould, N.A. Johnson, R.B. Morland, Inorg. Chem. 15 (1976) 1929.
[23] B.A. Barshop, R.F. Wrenn, C. Frieden, Anal. Biochem. 130 (1983) 134.
[24] G.A.K. Thompson, A.G. Sykes, Inorg. Chem. 15 (1976) 638.
[25] L. Kiriazis, R. Mattes, Z. anorg. allg. Chem. 593 (1991) 90.
[26] B.B. Dhar, E.S. Gould, Dalton Trans. 14 (2007) 1416.
[27] B.B. Dhar, E.S. Gould, Inorg. Chim. Acta 362 (2009) 188.
[28] Z. Yang, E.S. Gould, Dalton Trans. 2 (2006) 396.
[29] D.E. Linn Jr., S.K. Ghosh, E.S. Gould, Inorg. Chem. 28 (1989) 3225.
[30] M. Ardon, A. Pernick, Inorg. Chem. 12 (1973) 2484.
[31] G.R. Gayley, R.S. Taylor, R.K. Wharton, A.G. Sykes, Inorg. Chem. 16 (1977) 1377.
[32] P. Chalipoyil, F.C. Anson, Inorg. Chem. 17 (1978) 2418.
[33] M.T. Paffett, F.C. Anson, Inorg. Chem. 20 (1981) 3967.
[34] Z. Yang, E.S. Gould, Dalton Trans. 28 (2006) 3427.
[35] A. Keller, J.M. Sobczak, J.J. Ziolkowski, in: E.R. Braithwaite, J. Haber (Eds.), Molybdenum: An Outline of its Chemistry and Uses, Elsevier, Amsterdam, 1994 (ch. 11 See, for example).
[36] R.N. Bose, E.S. Gould, Inorg. Chem. 24 (1985) 2645 (2832).
[37] (a) J.C. Chen, E.S. Gould, J. Am. Chem. Soc. 95 (1973) 5198;
(b) B.R. Baker, M. Orhanovic, N. Sutin, J. Am. Chem. Soc. 89 (1967) 722.
[38] R.T.M. Fraser, R.G. Miller, V.W. Cope, Coord. Chem. Rev. 1 (1966) 85.
[39] B.B. Dhar, R. Mukherjee, E.S. Gould, Dalton Trans. 5 (2009) 868.
[40] W. Watanabe, F.H. Westheimer, J. Chem. Phys. 17 (1949) 61.
[41] (a) M.C. Ghosh, E.S. Gould, Inorg. Chem. 30 (1991) 491;
(b) M.C. Ghosh, E. Gelerinter, E.S. Gould, Inorg. Chem. 30 (1991) 1039.
[42] S.I. Scott, A. Bakac, J.H. Espenson, J. Am. Chem. Soc. 114 (1991) 4205.
[43] (a) S.K. Chandra, E. Gelerinter, E.S. Gould, Inorg. Chem. 34 (1995) 4057;
(b) S.K. Chandra, E.S. Gould, Res. Chem. Intermed. 22 (1996) 43.
[44] O.A. Babich, E.S. Gould, Inorg. Chem. 43 (2004) 1779.
[45] E.S. Gould, Coord. Chem. Rev. 135 (1994) 651.
[46] R.N. Bose, N. Rajasekar, D.N. Thompson, E.S. Gould, Inorg. Chem. 25 (1986) 3349.
[47] S.K. Ghosh, R.N. Bose, E.S. Gould, Inorg. Chem. 26 (1987) 2684.
[48] S.K. Ghosh, R.N. Bose, E.S. Gould, Inorg. Chem. 26 (1987) 2688.
[49] J.H. Espenson, J. Am. Chem. Soc. 86 (1964) 5101.
[50] L. Ciavatta, A. Pirozzi, Polyhedron 2 (1983) 769.
[51] B.B. Dhar, E.S. Gould, Dalton Trans. 39 (2010) 1616.
[52] J.P. Fackler Jr., Encyclopedia of Inorganic Chemistry, 2nd edn., Wiley, New York, 2006, p. 1.
[53] S.M. Wang, S.J. Hwu, J.A. Paradis, M.H. Whangbo, J. Am. Chem. Soc. 117 (1995) 5515.
[54] J.M.B. Van Colbe, M. Felderhoff, B. Bogdanovic, F. Schmitt, C. Weidenthaler, Chem. Commun. 37 (2005) 4732.
[55] F. Pohlki, S. Doye, Chem. Soc. Rev. 32 (2) (2003) 104.